Divalent Cations Stabilize the α1β1 Integrin I Domain†

Philip J. Gotwals,*,‡ Gloria Chi-Rosso,‡ Sarah T. Ryan,‡ Irene Sizing,‡ Mohammad Zafari,‡ Chris Benjamin,‡ Jus Singh,‡ Sergei Yu. Venyaminov,§ R. Blake Pepinsky,‡ and Victor Koteliansky‡

Biogen, Inc., 14 Cambridge Center, Cambridge, Massachusetts 02142, and Department of Biochemistry and Molecular Biology, Mayo Foundation, 200 First Street SW, Rochester, Minnesota 55905

Received December 3, 1998; Revised Manuscript Received April 21, 1999

ABSTRACT: Recent structural and functional analyses of α integrin subunit I domains implicate a region in cation and ligand binding referred to as the metal ion-dependent adhesion site (MIDAS). Although the molecular interactions between Mn^{2+} and Mg^{2+} and the MIDAS region have been defined by crystallographic analyses, the role of cation in I domain function is not well understood. Recombinant α1β1 integrin I domain (α1-I domain) binds collagen in a cation-dependent manner. We have generated and characterized a panel of antibodies directed against the α1-I domain, and selected one (AJH10) that blocks α1β1 integrin function for further study. The epitope of AJH10 was localized within the loop between the α3 and α4 helices which contributes one of the metal coordination sites of the MIDAS structure. Kinetic analyses of antibody binding to the I domain demonstrate that divalent cation is required to stabilize the epitope. Denaturation experiments demonstrate that cation has a dramatic effect on the stabilization of the I domain structure. Mn^{2+} shifts the point at which the I domain denatures from 3.4 to 6.3 M urea in the presence of the denaturant, and from 49.5 to 58.6 °C following thermal denaturation. The structural stability provided to the α1-I domain by divalent cations may contribute to augmented ligand binding that occurs in the presence of these cations.

Integrins are heterodimeric, cell surface proteins involved in cell−cell and cell−matrix adhesion and signal transduction (*2*). The integrin family is comprised of 8 β subunits and 17 α subunits. The integrin α1β1 is expressed on a variety of cell types, including those of hematopoietic, neuronal, and mesenchymal origin, and can serve as a receptor for laminin and collagens (*3*−*5*). The interaction between α1β1 integrin and collagen promotes cell survival and proliferation (*6*, *7*), and regulates the expression of gene products involved in extracellular matrix remodeling (*8*). α1 belongs to a subset of α integrin subunits which contain a 200 amino acid inserted ("I") domain within their extracellular region. The epitopes of the majority of mAbs that block I domain-containing integrin function, including those that block α1β1 integrin function, lie within the I domain, implicating this region in ligand binding (*9*−*12*). Furthermore, recombinant I domains recapitulate the activity of the native integrins (*13*−*17*). For example, the α1β1 I domain specifically binds collagen and laminin with a K_D similar to that measured for purified, intact α1β1 (*9*). The presence of divalent cation is required for both native integrin and recombinant I domain binding to ligand.

Recent crystal structure analyses of integrin I domains demonstrate that they adopt a dinucleotide-binding fold, with a central parallel β sheet surrounded on both sides by α helices (*1*, *18*−*21*). A cation coordination sphere is located at the COOH-terminal end of the β-sheet, and mutations in any of the metal-coordinating side chains of the I domain abolish ligand binding (*22*−*25*). This functional region is referred to as the *m*etal *i*on-*d*ependent *a*dhesion *s*ite or MIDAS[1] (*1*). The five residues that coordinate the metal ion (DxSxS−T−D)[2] are completely conserved among I domains. Typically, the two serines and the COOH-terminal aspartic acid directly coordinate the metal ion, while the NH_2-terminal aspartic acid and the threonine interact indirectly with the cation via hydrogen bonds to water molecules.

Although the structural details of the interaction between Mn^{2+}/Mg^{2+} and the I domain have been elucidated, the role of divalent cation in ligand binding to the integrin I domain is not understood. One suggestion is that cation acts as a bridge between the I domain and ligand. In the crystal structure of the αM I domain bound with Mg^{2+}, a glutamate from a neighboring molecule completes the octahedral coordination sphere of the bound cation, leading the authors to suggest that this residue is a ligand mimetic (*18*). An analogous interaction has not been observed in other I domain structures, and to date no group has successfully crystallized an I domain with its ligand. Thus, whether there is a direct

† S.Y.V. is supported by NIH Grant GM34847 to Dr. Franklyn G. Prendergast (Mayo Foundation, Rochester, MN).

* Address correspondence to this author at Biogen, Inc., 14 Cambridge Center, Cambridge, MA 02142. Telephone: 617-679-2218. Fax: 617-679-3148. Email: philip_gotwals@biogen.com.

‡ Biogen, Inc.

§ Mayo Foundation.

[1] Abbreviations: MIDAS, metal ion-dependent adhesion site; CDR, complementarity-determining region; PCR, polymerase chain reaction; GST, glutathione-*S*-transferase; BSA, bovine serum albumin; FACS, fluorescence-activated cell sorter; FCS, fetal calf serum; EDTA, ethylenediaminetetraacetic acid.

[2] There are 68 residues between the DxSxS sequence and the threonine in the αL, αM, and αX I domains; 69 in the α1 and α2 I domains. A total of 32 residues separate the threonine and the NH_2-terminal aspartic acid in all integrin I domains (*1*). For clarity, we will refer to this conserved motif as (DxSxS−T−D).

10.1021/bi982860m CCC: $18.00
Published on Web 06/11/1999

interaction between cation and the integrin ligand remains controversial. Alternatively, divalent cations may induce local changes in the tertiary structure of the MIDAS region, or change the surface charge on the face of the I domain resulting in ligand binding. Current data do not distinguish between these models, nor are they mutually exclusive.

To further probe the structure of the I domain, we have generated a panel of mAbs directed against the α1β1 integrin I domain (α1-I domain). The mAbs derived from this screen fall into two classes: those that block and those that do not block α1β1 function. Sequence analyses of the complementarity-determining regions (CDRs) demonstrate that those mAbs that block function are clonally related, and we have chosen one (AJH10) for further analysis. The epitope of AJH10 lies within the loop between helices α3 and α4 which forms part of the MIDAS structure, and the affinity of AJH10 for this epitope is effected by cation. Denaturation studies demonstrate that cation is required not only for local stability of the MIDAS region, but also for stabilization of I domain secondary and tertiary structure. Thus, in contrast to recent crystallographic studies showing little or no effect of divalent cations on I domain structure (*26*), our data suggest that divalent cations may provide structural stability to the I domain.

EXPERIMENTAL PROCEDURES

Cloning and Mutagenesis of the α1-I Domain. Human and rat α1β1 integrin I domain sequences were amplified from full-length cDNAs (*24*, *27*) by the polymerase chain reaction (PCR) (PCR CORE Kit; Boehringer Mannheim, GmbH Germany), using either human-specific [5′-CAGGATCCG-TCAGCCCCACATTTCAA-3′ (forward); 5′-TCCTCGA-GGGCTTGCAGGGCAAATAT-3′ (reverse)] or rat-specific [5′-CAGGATCCGTCAGTCCTACATTTCAA-3′ (forward); 5′-TCCTCGAGCGCTTCCAAAGCGAATAT-3′ (reverse)] primers. The resulting PCR-amplified products were purified, ligated into pGEX4t-i (Pharmacia), and transformed into competent DH5α cells (Life Technologies). Ampicillin-resistant colonies were screened for the expression of the ∼45 kDa glutathione-*S*-transferase−I domain fusion protein. The sequences from inserts of plasmid DNA of clones that were selected for further characterization were confirmed by DNA sequencing.

A rat/human chimeric α1-I domain (RΔH) was generated (MORPH Mutagenesis kit; 5 prime − 3 prime), exchanging the rat residues G92, R93, Q94, and L97 (Figure 4) for the corresponding human residues, V, Q, R, and R, respectively. Clones harboring the RΔH I domain were identified by the loss of a diagnostic *Stu*I restriction enzyme site, and the inserts were confirmed by DNA sequencing.

Purification of α1-I Domains. The α1-I domains were expressed in *E. coli* as GST fusion proteins containing a thrombin cleavage site at the junction of the sequences. The clarified supernatant from cells lysed in PBS was loaded onto a glutathione Sepharose 4B column (Pharmacia) which was washed extensively with PBS. The α1-I domain−GST fusion protein was eluted with 50 mM Tris-HCl, pH 8.0, 5 mM glutathione (reduced). For denaturation studies, the I domain was cleaved with thrombin in 50 mM Tris, pH 7.5, and purified from the GST fusion partner. DTT was added to 2 mM, and the sample was loaded on a glutathione Sepharose 4B column. The flow-through and wash fractions were pooled and loaded onto a Q Sepharose FF column (Pharmacia). The α1-I domain was eluted with 50 mM Tris-HCl, pH 7.5, 10 mM 2-mercaptoethanol, 75 mM NaCl. The purified I domain displayed its predicted mass (24 871 Da) by electrospray ionization-mass spectrometry (ESI-MS), migrated as a single band by SDS−PAGE, and the protein eluted as a single peak of appropriate size by size exclusion chromotography on a Superose 6 FPLC column (Pharmacia).

I Domain Functional Analysis. 96 well plates were coated overnight at 4 °C with 1 μg/mL collagen IV (Sigma) or collagen Type I (Collaborative Biomedical), washed with Triton buffer (0.1% Triton X-100, 1 mM $MnCl_2$, 25 mM Tris-HCl, 150 mM NaCl), and blocked with 3% bovine serum albumin (BSA) in 25 mM Tris-HCl, 150 mM NaCl (TBS). Serial dilutions of the α1-I domain−GST fusion protein in TBS containing 1 mM $MnCl_2$ and 3% BSA were incubated on the coated plates at room temperature for 1 h, and washed in Triton buffer. Bound α1-I domain was detected with serial additions of 10 μg/mL biotinylated anti-GST polyclonal antibody (Pharmacia), ExtrAvidin−horseradish peroxidase (Sigma) diluted 1:3000 in TBS containing 1 mM $MnCl_2$ and 3% BSA, and 1-Step ABTS [2,2′-azinobis-(3-ethylbenzothiazoline sulfonate); Pierce]. Plates were read at OD_{405} on a microplate reader (Molecular Devices).

Generation of Anti-α1-I Domain Monoclonal Antibodies. Female Robertsonian mice (Jackson Labs) were immunized intraperitoneally (i.p.) with 25 μg of purified human α1β1 (*4*) emulsified with complete Fruend's adjuvant (LifeTechnologies). They were boosted 3 times i.p. with 25 μg of α1β1 emulsified with incomplete Freunds's adjuvant (LifeTechnologies). The mouse with the highest anti-α1-I domain titer was boosted i.p. with 100 μg of α1β1 3 days prior to fusion, and intravenously with 50 μg of α1β1 1 day prior to fusion. Spleen cells were fused with FL653 myeloma cells at a 1:6 ratio and were plated at 100 000 and 33 000 per well into 96 well tissue culture plates.

Supernatants were assessed for binding to the α1β1 integrin by single-color FACS. Prior to FACS analysis, supernatants were incubated with untransfected K562 cells to eliminate IgG that bound solely to the β subunit. Subsequently, $3-5 \times 10^4$ K562 cells transfected with the α1 integrin subunit (K562-α1) suspended in FACS buffer [1% fetal calf serum (FCS) in PBS containing 0.5% NaN_3] were incubated with supernatant for 45 min at 4 °C, washed, and incubated with anti-mouse IgG conjugated to phycoerythrin. After washing twice with FACS buffer, cells were analyzed in a Becton Dickinson flow cytometer.

Supernantants from the resulting hybridomas were screened for binding to the α1-I domain. Briefly, 50 μL of 30 μg/mL human α1-I domain−GST fusion in PBS was coated onto wells of a 96 well plate (Nunc) overnight at 4 °C. The plates were washed with PBS and blocked with 1% BSA in PBS, and the hybridoma supernatant was incubated with the I domain at room temperature for 1 h. After extensive washing with PBS containing 0.03% Tween 20, alkaline phosphatase-linked anti-mouse IgG (Jackson ImmunoResearch) was added for an additional hour. After a final wash, 1 mg/mL *p*-nitrophenyl phosphate (*p*NPP) in 0.1 M glycine, 1 mM $ZnCl_2$, and 1 mM $MgCl_2$ was added for 30 min at room temperature, and the plates were read at OD_{405}.

Selected supernatants were tested for their ability to inhibit K562-α1-dependent adhesion to collagen IV. K562-α1 cells were labeled with 2 mM 2′,7′-bis(2-carboxyethyl-5(and 6)-carboxyfluorescein) pentaacetoxy methyl ester (BCECF; Molecular Probes) in DMEM containing 0.25% BSA at 37 °C for 30 min. Labeled cells were washed with binding buffer (10 mM Hepes, pH 7.4, 0.9% NaCl, and 2% glucose) and resuspended in binding buffer plus 5 mM $MgCl_2$ at a final concentration of 1×10^6 cells/mL. Fifty microliters of supernatant was incubated with an equal volume of 2×10^5 K562-α1 cells in wells of a 96 well plate. The plate was then centrifuged, and the supernatants were removed. Cells were resuspended in binding buffer and transferred to wells of a collagen-coated plate and incubated for 1 h at 37 °C. Following incubation, the nonadherent cells were removed by washing 3 times with binding buffer. Attached cells were analyzed on a Cytofluor (Millipore).

Immunoblotting. The smooth muscle cell layer dissected from sheep aorta and K562-α1 cells were extracted with 1% Triton X-100 in 50 mM Hepes, pH 7.5, 150 mM NaCl, 10 mM phenylmethylsulfonyl flouride (PMSF), 20 μg/mL aprotinin, 10 μg/mL leupeptin, and 10 mM ethylenediaminetetraacetic acid (EDTA). Samples were subjected to 4−20% gradient SDS−PAGE, and electroblotted onto nitrocellulose membranes. The blots were blocked with 5% dry milk in TBS, washed in TBS containing 0.03% Tween-20, and incubated with antibodies in blocking buffer containing 0.05% NaN_3 for 2 h. Blots were then washed as before, incubated with horseradish peroxidase-conjugated anti-mouse IgG for 1 h, washed again, and then treated with ECL reagent (Amersham). Blots were then exposed to film (Kodak) for 30−60 s, and developed.

Sequencing of the Complementarity-Determining Regions. Two micrograms of mRNA, isolated from 10^7 hybridomas (FastTrack mRNA isolation kit, Invitrogen), was reverse-transcribed (Ready-To-Go You Prime First Strand Kit, Pharmacia Biotech) using 25 pM each of the following primers: heavy chain, VH1FOR-2 (*28*); light chain, VK4FOR, which defines four separate oligos (*29*). For each hybridoma, heavy and light chains were amplified in four separate PCR reactions using various combination of the following oligos: (1) heavy chain: VH1FR1K (*30*), VH1BACK, VH1BACK (*31*), $V_H$fr1a, $V_H$fr1b, $V_H$fr1e, $V_H$fr1f, $V_H$fr1g (*32*), or VH1FOR-2 (*28*); (2) light chain: VK1BACK (*31*), VK4FOR, VK2BACK oligos (*29*), or $V_K$fr1a, $V_H$fr1c, $V_H$fr1e, $V_H$fr1f (*32*). Products were amplified (5 min at 95 °C, 50 cycles of 1 min at 94 °C, 2 min at 55 °C, 2 min at 72 °C, and a final cycle of 10 min at 72 °C), gel-purified (QIAquick, Qiagen), and sequenced directly using various listed oligos on an ABI 377 Sequencer.

BIACore Analysis. All experiments were performed at 25 °C with a 10 μL/min flow rate on a BIAcore 2000 biosensor system (BIAcore, Inc.). The CM5 chip surface was first activated with *N*-hydroxysuccinimide/*N*-ethyl-*N*′-(3-diethylaminopropyl)carbodiimide hydrochloride (BIAcore, Inc.), coupled with goat anti-mouse IgG:Fc specific [30 μg/mL in 10 mM acetic acid (pH 4); Jackson ImmunoResearch], and blocked with ethanolamine hydrochloride (pH 8.5). The chip was regenerated 5 times with 20 μL of 1 mM formic acid to establish a base line (1500 resonance units). For each experiment, 250 μL of function-blocking anti-α1-I domain mAb (30 μg/mL) in HBS buffer (10 mM HEPES, 150 mM NaCl, and 0.005% P20 surfactant, pH 7.4) was injected over the surface of the chip. The chip was washed, and 250 μL of human I domain (30 μg/mL) in the presence of either 1 mM $MgCl_2$, 1 mM $MnCl_2$, or 3.4 mM EDTA was injected, followed by a second wash. The surface was regenerated between experiments by injecting 30 μL of 1 mM formic acid. Data analyses were performed using BIAevaluation 2.1 software (BIAcore, Inc.).

Denaturation Studies. The denaturation of the α1-I domain as a function of urea was measured by fluorescence spectroscopy in an Aminco-Bowman series 2 luminescence spectrometer. Samples containing 0.6 μM α1-I domain in 50 mM Tris-HCl, pH 7.0, 0.15 mM DTT with no addition, 1 mM $CaCl_2$, or 1 mM $MnCl_2$ and with varying amounts of urea were analyzed at 25 °C using an excitation wavelength of 280 nm. Emission spectra from 300 to 400 nm were collected. Fluorescence data at 350 nm were plotted as a function of urea and standardized using the change in fluorescence from 0 to 9 M urea for each of the test conditions as a measure of the total fraction folded.

Circular Dichroism. Circular dichroism spectra were recorded using a J-710 spectropolarimeter (JASCO, Japan) equipped with a programmable temperature water bath (CTC-345, JASCO). Far-UV (185−250 nm) and temperature-dependent measurements were performed using U-type cells of path length 0.0148 cm and volume 0.045 mL with α1-I domain in 20 mM HEPES, 1 mM EDTA, 1 mM DTT, pH 7.5, in the absence of divalent cations, or the presence of either 2 mM Mg^{2+} or Mn^{2+} at a protein concentration of 55 μM. CD spectra were recorded using a scan speed of 20 nm/min, a response time of 2 s, and a bandwidth of 2 nm. Temperature-dependent measurements were performed in the range 10−80 °C. The continuous temperature scan at fixed wavelength (222 nm) in the far-UV range was done using a scan rate of 50 °C/h and a response time of 8 s. Data are presented as molar ellipticity per residue.

Structural Modeling of the α1-I Domain. A homology model of the human α1-I domain was built using the X-ray crystal structure of the human α2-I domain (*19*). The model was built using the homology modeling module of Insight II (version 2.3.5; Biosym Technologies). The program CHARMM (*33*) was used with the all-hydrogen parameter set 22 with a distant-dependent dielectric constant of 2 times the atom separation distance. We first did 1000 steps of steepest descent minimization with mass-weighted harmonic positional constraints of 1 kcal/(mol·Å^2) on all atoms of the α1-I domain. This minimization was followed by another 1000 steps of steepest descent and 5000 steps of Adopted-Basis Newton Raphson with constraints of 0.1 kcal/(mol·Å^2) on the C-α atoms of the α1-I domain to avoid significant deviations from the α2-I domain X-ray crystal structure.

RESULTS

Binding of the α1-I Domain to Collagen Is Divalent Cation-Dependent. The human and rat (95% identity to human) α1-I domains were expressed in *E. coli* as GST-fusion proteins and purified over glutathione Sepharose. Both proteins were examined for binding to collagens I and IV using a variation of an ELISA-based assay previously described (*9*). The human α1-I domain binds collagen IV

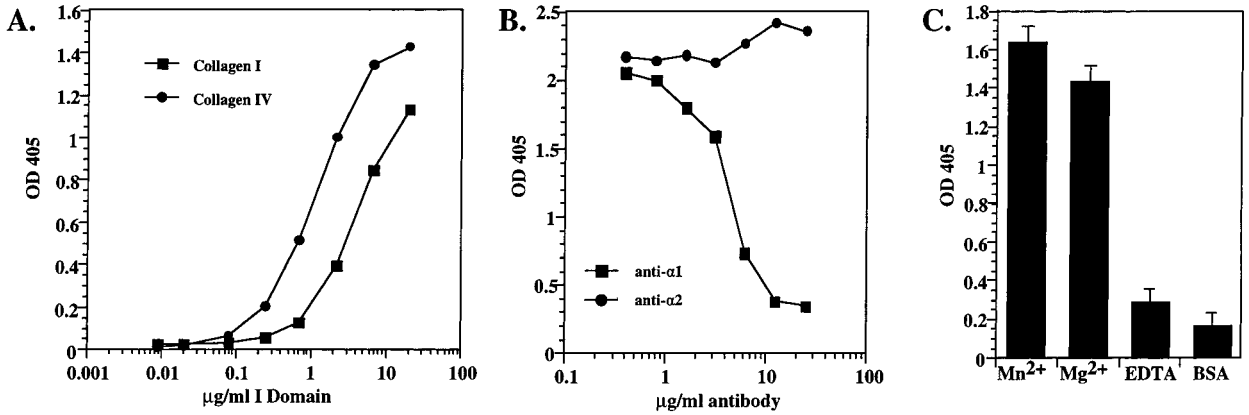

FIGURE 1: The α1-I domain binds collagen. (A) Increasing concentrations of the human α1-I domain were bound to plates previously coated with 1 μg/mL collagen I (squares) or collagen IV (circles). Values shown have been corrected for background binding to BSA. (B) 2 μg/mL human α1-I domain was mixed with increasing concentration of an anti-human α1 integrin antibody 5E8D9 (squares) or an anti-human α2 integrin antibody A2IIE10 (circles), and then bound to plates previously coated with 1 μg/mL collagen IV. (C) Plates were coated with 1 μg/mL collagen IV or 3% BSA. α1-I domain (2 μg/mL) was subsequently bound to coated plates in the presence of 1 mM Mn^{2+}, 1 mM Mg^{2+}, or 5 mM EDTA. Data shown are representative of three independent experiments.

with better efficiency than collagen I (Figure 1A). An antibody specific to the α1-I domain, but not an antibody specific to the α2-I domain (Figure 1B), abrogated binding to both ligands (data for collagen I are not shown). Both Mn^{2+} and Mg^{2+} stimulated binding, and EDTA reduced binding to background levels (Figure 1C). No measurable differences in ligand binding were detected between the human and rat α1-I domains, suggesting that the sequence differences between species are not functionally relevant (data not shown). Thus, our data corroborate the published literature that I domains, in general, and that the α1-I domain, specifically, require cation for efficient ligand binding.

Generation of mAbs Specific to the α1-I Domain. Monoclonal antibodies have proved to be very useful probes in studying the relationship between structure and function of integrin subunits. For example, mAbs were used extensively to study regions of the β1 subunit associated with an activated conformation (*34*). Thus, to identify potential probes for conformational changes of the α1-I domain, we generated a panel of mAbs to the human α1-I domain. We initially identified 19 hybridomas, the supernatants of which bound to human leukemia K562 cells expressing the α1β1 integrin (K562-α1) and to the α1-I domain. The immunoglobulins were purified from each of these hybridomas and tested for the ability to block either K562-α1 or α1-I domain binding to collagen IV. The mAbs fall into two classes: those that block and those that do not block α1β1 function. For example, while the mAbs produced by clones AEF3, BGC5, and AJH10 bind the α1-I domain (Figure 2A, data not shown for BGC5), only mAb AJH10 inhibits α1-I domain-dependent (Figure 2B) or K562-α1 (Figure 2C) adhesion to collagen IV.

To establish the clonal origin of this panel of mAbs, we amplified by PCR and sequenced the CDRs from 12 of the 19 antibodies (data not shown). Sequences from clones producing function-blocking mAbs were nearly identical across all the complementarity-determining regions (CDRs) and the intervening framework regions, suggesting that these hybridomas are clonally related. Sequences of the variable regions of the nonblocking antibodies were markedly different from the clonally related family of sequences found for the blocking antibodies. As the blocking antibodies appear to originate from a single clone, we chose one (AJH10) to characterize further. Immunoblotting (Figure 3A) and FACS analysis (Figure 3B) demonstrate that AJH10 reacts with human, rabbit, and sheep, but not rat, α1β1 integrin, suggesting that the blocking mAbs bind to an evolutionarily conserved, linear epitope. These mAbs should prove useful in deciphering α1β1 integrin function in a variety of mammalian species. The nonblocking mAbs were neither efficient at immunoblotting nor did they react with species other than human.

A Cation-Dependent Epitope Resides Near the MIDAS Motif. We exploited the observation that AJH10 recognizes the human, but not the rat, α1-I domain sequences to map the epitope for the α1β1 function-blocking mAbs. The human and rat sequences differ by only 12 amino acids, 4 of which lie in a stretch of 6 amino acids (aa 92−97, Figure 4A) adjacent to the critical threonine (Figure 4A, aa 98) within the MIDAS motif. To test the hypothesis that these residues comprise the epitope for the blocking mAbs, we constructed a chimeric I domain (RΔH), exchanging the rat residues G92, R93, Q94, and L97 for the corresponding human residues, V, Q, R, and R, respectively. AJH10, along with all the function-blocking mAbs, recognizes the chimeric I domain (RΔH; Figure 4B).

To orient these residues with respect to the MIDAS domain in the tertiary structure of the α1-I domain, we modeled the α1-I domain using the coordinates of the crystal structure of the α2-I domain. The α1 and α2 integrin sequences exhibit 51% identity with no insertions or deletions, suggesting that the overall structure of the two I domains will be similar. The metal coordination site is predicted to be the same in the α1-I domain as in the α2-I domain, and the residues that comprise the epitope for the blocking mAbs lie on a loop between helix α3 and helix α4 which contains the threonine within the MIDAS motif critical for cation binding (Figure 5). The α1-I domain model predicts that the amide nitrogen of Q92 (Figure 4A) hydrogen bonds with the carbonyl group of I33, the residue adjacent to S32 (Figure 5). Thus, the loop that contains the epitope may play a functional role in stabilizing the MIDAS region.

The proximity to and the potential interaction of the loop containing the epitope with the MIDAS motif suggested that

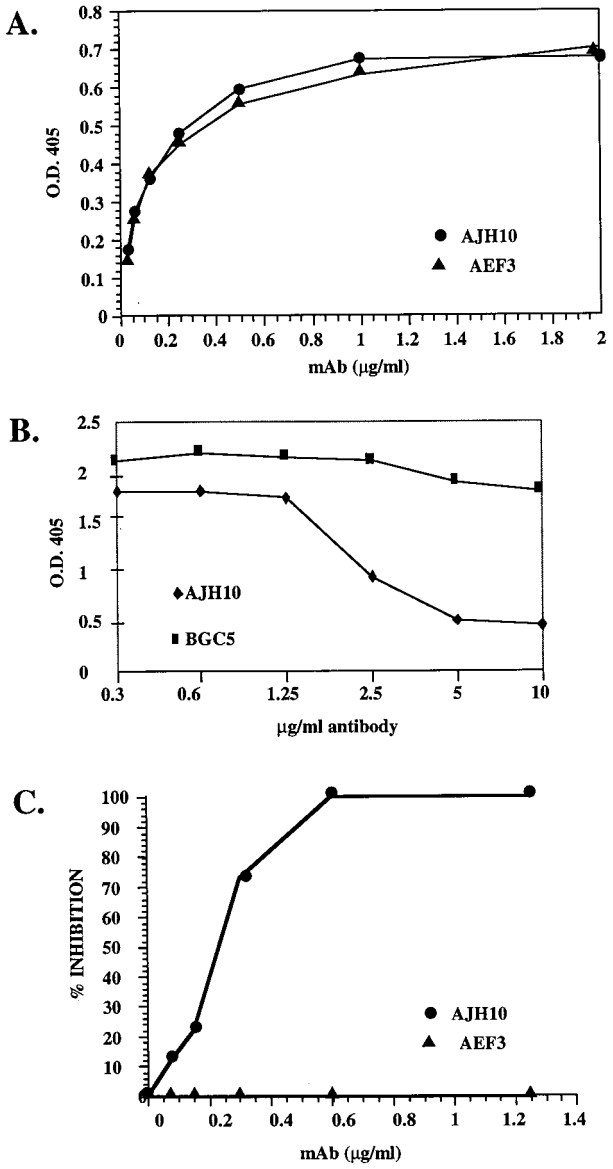

FIGURE 2: Identification of a blocking mAb to the α1-I domain. (A) Increasing concentrations of mAbs AEF3 (triangles) or AJH10 (circles) were bound to plates coated with 30 μg/mL α1-I domain. (B) The α1-I domain was treated with increasing concentrations of mAb AJH10 (diamonds) or mAb BGC5 (squares) and bound to collagen IV (2 μg/mL) coated plates. (C) K562-α1 cells were treated with increasing concentration of mAbs AEF3 (triangles) or AJH10 (circles) and bound to collagen IV (5 μg/mL) coated plates. A total of 45−50% of the cells added to each well adhered to collagen IV. Data shown are representative of three independent experiments.

the epitope, itself, might be sensitive to the presence of divalent cation. Initial ELISA-based experiments confirmed that binding of AJH10, but not AEF3 (Figure 6A), to purified α1β1 integrin increases in the presence of cations. Binding of AJH10 to cell surface-expressed α1β1 is also enhanced by the addition of cation (Figure 6B). To further analyze this observation, we measured the relative binding affinities of the blocking mAbs, in the presence or absence of divalent cations, using a surface plasmon resonance (SPR) biosensor. Monitoring the reversible binding of the mAbs to the recombinant α1-I domain in real time allows the derivation of the association (k_a) and dissociation rates (k_d), as well as the corresponding apparent dissociation constants (K_D). The addition of cation decreased the K_D of blocking mAb AJH10 from 400 to 20 nM (Table 1). The addition of cation had no effect on the K_D of nonblocking, control mAb AEF3 (Table 1, legend). Analysis of the k_a and k_d associated with binding reveals that the increase in affinity is primarily attributable to a decrease in the rate of dissociation (Table 1). For example, in the absence of cation, AJH10 has a dissociation rate constant of 1.65×10^{-3}/s. Addition of Mn^{2+} decreases the dissociation rate constant by a factor of 8 to 2.12×10^{-4}/s (Table 1) while increasing the association rate by only a factor of 2 (3.9×10^3 M^{-1} s^{-1} to 8.0×10^3 M^{-1} s^{-1}). Thus, the addition of divalent cation appears to stabilize the epitope rather than unmask a cryptic site, consistent with the proximity of the epitope to the MIDAS region.

Table 1: Biacore Analysis of Blocking mAb AJH10[a]

	K_D ($\times 10^{-7}$ M)		k_a ($\times 10^3$ M^{-1} s^{-1})		k_d ($\times 10^{-3}$ s^{-1})	
	−	+	−	+	−	+
Mg^{2+}	2.88	0.36	3.78	7.75	1.09	0.276
Mn^{2+}	4.23	0.26	3.90	8.02	1.65	0.212

[a] (−): no cation, in the presence of EDTA; (+): in the presence of 1 mM cation. The K_D of nonblocking, control mAb AEF3 was 15 nM, in the presence of Mg^{2+}, and 18 nM, in the absence of Mg^{2+}.

Cation Is Required for I Domain Stability. One interpretation of the effect Mn^{2+} and Mg^{2+} have on epitope expression is that divalent cations are required to stabilize the MIDAS region, or the entire α1-I domain. Thus, we looked at the stability of the α1-I domain in the presence or absence of cations under denaturing conditions.

The presence of divalent cations had a stabilizing effect on the α1-I domain structure readily detected by measuring the susceptibility of the protein to denaturation by urea (Figure 7). Denaturation of the α1-I domain was assessed by monitoring the change in intrinsic fluorescence that results from the exposure of buried tryptophan and tyrosine residues to the aqueous environment as the protein unfolds. Denaturation produced both an increase in fluorescence intensity and a red shift in the emission spectrum. The maximal effect was seen at 360 nm where denaturation of the α1-I domain resulted in a greater than 4-fold increase in intrinsic fluorescence intensity. In the absence of divalent cation, the α1-I domain was sensitive to the presence of low concentrations of urea, and the amount needed to produce a half-maximal change in fluorescence intensity was 3.4 M urea. In the presence of Mn^{2+}, half-maximal denaturation shifted to 6.3 M urea, indicating a substantial stabilization of the α1-I domain.

The output of the spectrophotometric data discussed above is determined primarily by the fluorescence of a single buried tryptophan, which lies within the MIDAS region of the α1-I domain (W36, Figure 4A). Thus, the spectrophotometric data only provide a view of the MIDAS region and not of the entire I domain.

To distinguish between local and possible wide-range effects on structure, we determined, by measuring circular dichroism spectra in the presence or absence of Mn^{2+} and Mg^{2+}, the temperature at which the I domain denatured, and the effect of denaturation on the secondary structure of the protein. Near- and far-UV CD spectra for the α1-I domain, in the presence and absence of cation at room temperature, were indistinguishable (data not shown). In contrast, large, cation-dependent differences were seen in the susceptibility

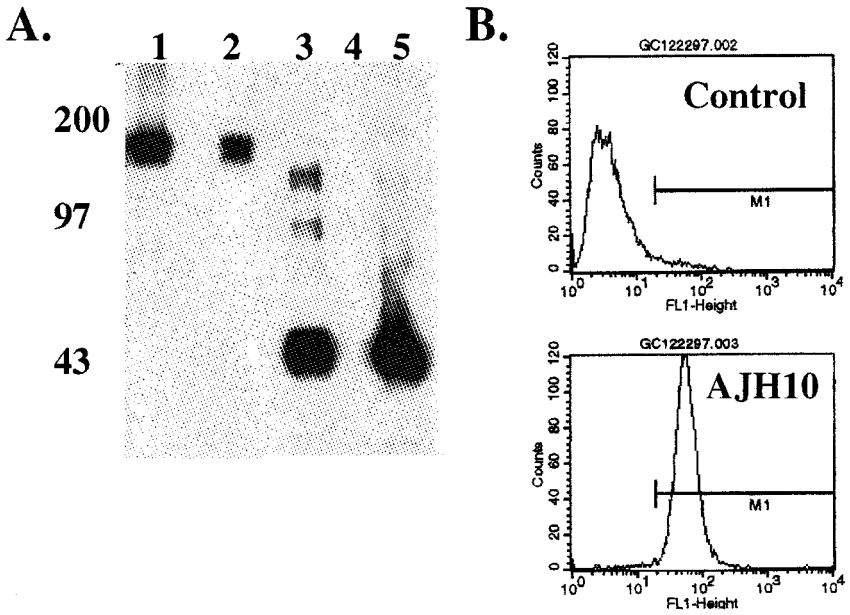

FIGURE 3: Species cross-reactivity of AJH10. (A) Detergent lysates from (1) sheep vascular smooth muscle, (2) human leukemia K562-α1 cells, (3) purified RΔH GST-I domain, (4) rat GST-α1-I domain; and (5) human GST-α1-I domain were separated by 10−20% SDS−PAGE under nonreducing conditions, and immunoblotted with function-blocking mAb AJH10. Molecular weight markers are shown on the left; nonreduced α1β1 integrin migrates at ∼ 180 kDa; GST-I domain migrates at ∼45 kDa. (B) Rabbit vascular smooth muscle cells were incubated with either mAb AJH10 (bottom) or murine IgG control (top) and analyzed by FACS.

of the I domain to thermal denaturation. In the absence of divalent cations, the I domain denatured at $T_m = 49.5$ °C. Both Mn^{2+} ($T_m = 58.6$ °C) and Mg^{2+} ($T_m = 54.6$ °C) stabilized the I domain as indicated by increases in T_m (Figure 8). Heat denaturation in the apo state was accompanied by a 20−25% decrease in ordered secondary structure at 65 °C. Decreases of 45% were observed for the Mn^{2+} state at 70 °C and of 34% for the Mg^{2+} state at 80 °C. For the apo state, CD spectra at 65 and 80 °C have minima which are characteristic of a high content of helical structure, whereas in the presence of divalent cations CD spectra at 70−80 °C have shapes that are characteristic for "aggregational" β structure. These data suggest that, in addition to the local stabilizing effect cations have on the MIDAS region, the presence of cations has a wide-ranging effect on the secondary structure of the α1-I domain. It is interesting to note that Mn^{2+} is more stabilizing than Mg^{2+} as evidenced by a greater shift in T_m. Since Mn^{2+} is more effective at promoting ligand binding to the α1β1 integrin (*35*), the stabilizing effects of Mn^{2+} may be related to the increased affinity of the I domain for ligand.

DISCUSSION

The molecular details of the interaction between conserved residues within the MIDAS motif (DxSxS−T−D) and Mg^{2+} or Mn^{2+} have recently been elucidated. Crystal structure analyses of three different I domains (αL, αM, α2) bound in the presence or absence of metal ion demonstrate that typically the two serine residues and the COOH-terminal aspartic acid directly coordinate the metal ion, while the threonine and the NH_2-terminal aspartic acid indirectly coordinate via hydrogen bonds to water molecules (*1*, *18*−*21*, *26*). The structural motif of all three crystals is conserved, and the addition of the metal ions had minimal effect on the overall structure of the motif. Despite the extensive structural data for metal binding, the functional relationship between cation and ligand binding is not well understood for any of the integrins.

A number of possibilities exist for which there is limited experimental data, of which two have received some attention. Integrin β subunits contain a MIDAS-like motif imbedded within a structure that has features reminiscent of an I domain and is associated with cation and ligand binding (*36*−*38*). Studies examining ligand and cation binding to a peptide derived from this MIDAS-like region from within the β3 subunit suggest that cation and ligand binding are mutually exclusive. These studies have led to the hypothesis that cation, ligand, and receptor form a ternary complex from which the cation is displaced during ligand binding (*39*). Data from a recent study examining the role of metal ion in ligand binding to the α2-I domain are consistent with this model. As observed with the β3 subunit peptide, initial ligand binding is cation-dependent, but the cation is subsequently displaced as a function of ligand binding (*40*).

Another explanation which has received attention is that the cation affects the local structure of the I domain to generate an "active" conformation. This hypothesis is based, in part, on considerable literature demonstrating that many native integrins require activation by some stimuli (of which Mn^{2+} is one) to bind ligand (*41*). For example, LFA-1 (integrin αLβ2) on resting leukocytes does not bind its ligands ICAM-1, -2, and -3, but can be activated to bind by a number of agents, including a monoclonal antibody that maps to the αL-I domain (*42*). This activating mAb may affect the structure of the I domain to permit ligand binding. There is, however, no structural data to suggest that metal ions directly affect the conformation of the MIDAS region. A comparison of the αL (*21*) and the αM I domains (*26*) crystallized in the presence of different metal ions revealed no major changes in the binding face of the I domain.

Our data, while they cannot exclude the former possibilities, suggest that cation is required for the maintenance of

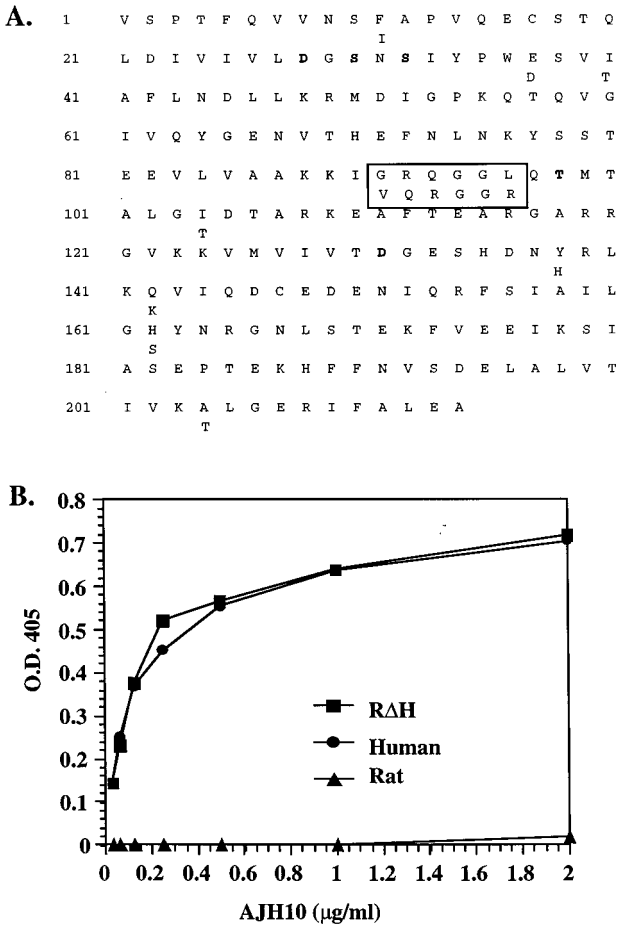

FIGURE 4: Location of the epitope for the anti-α1-I domain-blocking mAbs. (A) Amino acid sequences of the rat (top) and human (bottom) α1-I domains. The residues that comprise the MIDAS motif are shown in boldface type. The human amino acids that replaced the corresponding rat residues (RΔH) are shown below the rat sequence in the boxed region. For clarity, residue numbering in the text refers to this figure. (B) Increasing concentrations of mAb AJH10 were bound to plates coated with 30 μg/mL human (circles), rat (triangles), or RΔH (squares) α1-I domain. Data shown are representative of three experiments.

the overall structural integrity of the α1 integrin I domain. First, analysis of the kinetics of mAb binding to the α1-I domain suggests that in the presence of cation, the dissociation rate, and not the association rate, is preferentially effected, resulting in an increase in affinity. Thus, mAbs associated with the α1-I domain in the presence or absence of divalent cation, suggesting that the epitope is not masked. Rather, cation stabilizes the epitope, effectively lowering the dissociation rate. Second, the thermal and urea denaturation studies show that the presence of cation stabilizes the α1-I domain structure. In particular, data from circular dichroism spectra demonstrate that the increase in temperature required to unfold the α1-I domain in the presence of cations is accompanied by cation-dependent changes in the secondary structure.

It is possible that in the native integrin, the role of the cation is less critical to the structural integrity of the I domain. Regions of the integrin which contact the I domain could provide structural support. A recent structure prediction suggests that the intact integrin α subunit forms a β-propeller domain, and that the I domain exists as an associated, but structurally independent domain hinged between two folds

FIGURE 5: Structural model of the α1-I domain. Residues that comprise the MIDAS motif (DxSxS−T−D) are shown in magenta. For clarity, the COOH-terminal aspartic acid is omitted. The region of the epitope to which the α1-I domain function-blocking mAbs map is shown in red, and the residue Q92 which interacts with the MIDAS region is designated. The hydrogen bonding distance between Q92 and I33 is 2.8 Å. Note that the epitope lies on the same loop as T98. The yellow sphere represents the Mn^{2+} ion.

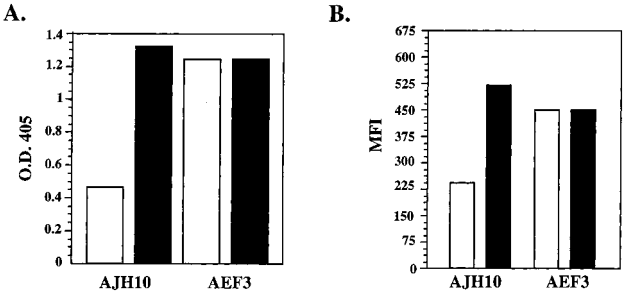

FIGURE 6: Cation stabilizes the expression of the epitope. (A) 0.5 μg of blocking mAb AJH10 or nonblocking mAb AEF3 in the presence of 5 mM EDTA (open bars) or 1 mM $MnCl_2$ (solid bars) was bound to plates previously coated with 1 μg/mL affinity-purified, human α1β1 integrin. (B) 5 μg/mL AJH10 or AEF3 was incubated with K562-α1 cells in the presence of 2 mM $MnCl_2$ (solid bars) or following a wash with 5 mM EDTA (open bars). Bound antibody was measured by FACS and is reported as the mean fluorescence intensity (MFI).

of the propeller. The implication of this model is that the structural integrity of the I domain does not necessarily depend on adjacent regions of the integrin α subunit (*43*). Our binding data with mAb AJH10 are consistent with this notion. Metal ions increased the binding of AJH10 not only to the α1-I domain but also to purified α1β1 integrin, and to α1β1 integrin expressed on the surface of cells.

Structural data suggesting that the I domain is, in fact, conformationally flexible come from an analysis of the αM-I domain which has recently been crystallized in the presence of Mn^{2+} or Mg^{2+} (*18*). Comparison of the two structures reveals a change in the metal coordination, significantly

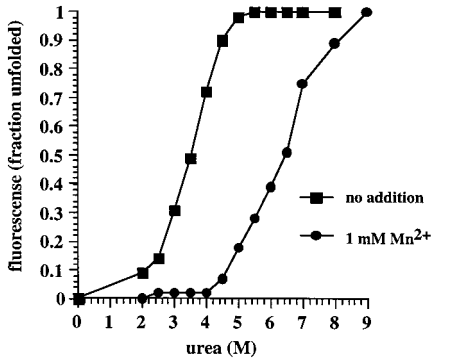

FIGURE 7: Denaturation of the α1-I domain by urea. 0.6 μM rat α1-I domain in the presence of no cation (squares) or with 1 mM $MnCl_2$ (circles) and increasing concentrations of urea was analyzed at 25 °C using an excitation wavelength of 280 nm. Fluorescence data from the emission spectra at 350 nm are plotted as a function of urea concentration and standardized using the change in fluorescence for each of the test conditions as a measure of the total fraction unfolded.

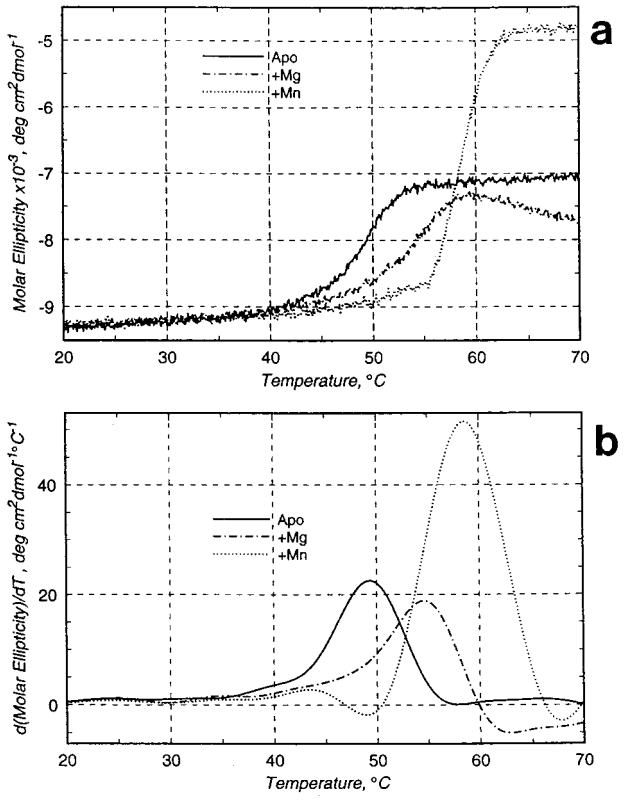

FIGURE 8: Circular dichroism spectra of thermally denatured α1-I domain. Temperature-dependent circular dichroism measurements at a fixed wavelength (222 nm) were performed using 55 μM α1-I domain in the absence (solid line) or presence of 2 mM Mg^{2+} (dot−dash line) or 2 mM Mn^{2+} (dotted line). Data are expressed as (a) continuous temperature dependence of molar ellipticity per residue and (b) first-derivative curves after smoothing the corresponding data curves shown in panel a.

altering the ligand binding surface of the I domain, and reducing the ability of the Mn^{2+}-bound αM-I domain to bind ligand-associated acidic residues. For example, one of the structural changes between these two crystal forms is a shift in the βA−α1 loop, which includes the DxSxS sequence, resulting in the threonine on the α3−α4 loop no longer directly coordinating the metal ion. The interpretation of these data is that in the Mg^{2+}-bound structure, a glutamic acid from a neighboring molecule acts as a ligand mimetic to complete the octahedral coordination site for the metal ion. The structural change may be due to a fortuitous crystal formation representing the "ligand-bound" state, rather than a direct effect of the species of metal ion. Other recent data also suggest that the I domain is flexible. Mutations in sites within the αM-I domain, but distinct from the MIDAS region, affect the activation state of the intact αMβ2 integrin, suggesting that events at one site within the I domain can be transmitted to and have an effect at a topologically distinct location (*44*).

In summary, we have generated a panel of mAbs to the α1-I domain. Those mAbs that block α1β1 integrin function map to a divalent cation-sensitive epitope within the MIDAS motif of the α1-I domain, and exhibit cation-dependent binding. Denaturation studies demonstrate that cation stabilizes the MIDAS region and that W36 is a useful probe for these effects. Circular dichroism measurements, under denaturing conditions, reveal that cation binding affects not just the local expression of the epitope, but stabilizes the secondary structure of the α1-I domain. The ability of divalent cations to reduce the intrinsically flexible structure of the α1-I domain provides a possible explanation for how cations augment ligand binding.

ACKNOWLEDGMENT

We thank Dr. Eugene Marcantonio (Columbia) for the human α1 integrin cDNA clone; Dr. Michael Ignatious (University of California, Berkeley) for the rat α1 integrin cDNA clone; Dr. Vladimir Belkin for purified α1β1 integrin; Dr. Robert Liddington (University of Leicester) for the coordinates of the α2-I domain crystal structure prior to release to the Brookhaven database; and Dr. Roy Lobb (Biogen) for stimulating discussions.

REFERENCES

1. Lee, J.-O., Rieu, P., Arnout, M. A., and Liddington, R. (1995) *Cell 80*, 631−638.
2. Hynes, R. O. (1992) *Cell 69*, 11−25.
3. Hemler, M. E., Jacobson, J. G., Brenner, M. B., Mann, D., and Strominger, J. L. (1985) *Eur. J. Immunol. 15*, 502−508.
4. Belkin, V. M., Belkin, A. M., and Koteliansky, V. K. (1990) *J. Cell Biol. 111*, 2159−2167.
5. Dubond, J.-L., Belkin, A. M., Syfrig, J., Thiery, J. P., and Koteliansky, V. E. (1992) *Development 116*, 585−600.
6. Pozzi, A., Wary, K. K., Giancotti, F. G., and Gardner, H. A. (1998) *J. Cell Biol. 142*, 587−594.
7. Wary, K. K., Mainiero, F., Isakoff, S. J., Marcantonio, E. E., and Giancotti, F. G. (1996) *Cell 87*, 733−743.
8. Langholz, O., Rockel, D., Mauch, C., Kozlowska, E., Bank, I., Krieg, T., and Eckes, B. (1995) *J. Cell Biol. 131*, 1903−1915.
9. Calderwood, D. A., Tuckwell, D. S., Eble, J., Kuhn, K., and Humphries, M. J. (1997) *J. Biol. Chem. 272*, 12311−12317.
10. Champe, M., McIntyre, B. W., and Berman, P. W. (1995) *J. Biol. Chem. 270*, 1388−1394.
11. Huang, C., and Springer, T. A. (1995) *J. Biol. Chem. 270*, 19008−19016.
12. Kamata, T., Puzon, W., and Takada, Y. (1994) *J. Biol. Chem. 269*, 9659−9663.
13. Kamata, T., and Takada, Y. (1994) *J. Biol. Chem. 269*, 26006−26010.
14. Muchowski, P. J., Zhang, L., Chang, E. R., Soule, H. R., Plow, E. F., and Moyle, M. (1994) *J. Biol. Chem. 269*, 26419−26423.
15. Rieu, P., Ueda, T., Haruta, I., Sharma, C. P., and Arnaout, M. A. (1994) *J. Cell Biol. 127*, 2081−2091.
16. Ueda, T., Rieu, P., Brayer, J., and Arnaout, M. A. (1994) *Proc. Natl. Acad. Sci. U.S.A. 91*, 10680−10684.

17. Tuckwell, D., Calderwood, D. A., Green, L. J., and Humphries, M. J. (1995) *J. Cell Sci. 108*, 1629−1637.
18. Lee, J.-O., Bankston, L. A., Arnout, M. A., and Liddington, R. C. (1995) *Structure 3*, 1333−1340.
19. Emsley, J., King, S. L., Bergelson, J. M., and Liddington, R. C. (1997) *J. Biol. Chem. 272*, 28512−28517.
20. Qu, A., and Leahy, D. J. (1995) *Proc. Natl. Acad. Sci. U.S.A. 92*, 10277−10281.
21. Qu, A., and Leahy, D. J. (1996) *Structure 4*, 931−942.
22. Edwards, C. P., Champe, M., Gonzalez, T., Wessinger, M. E., Spencer, S. A., Presta, L. G., Berman, P. W., and Bodary, S. C. (1995) *J. Biol. Chem. 270*, 12635−12640.
23. Michishita, M., Videm, V., and Arnaout, M. A. (1993) *Cell 72*, 857−867.
24. Kern, A., Briesewitz, R., Bank, I., and Marcantonio, E. E. (1994) *J. Biol. Chem. 269*, 22811−22816.
25. Kamata, T., Wright, R., and Takada, Y. (1995) *J. Biol. Chem. 270*, 12531−12535.
26. Baldwin, E. T., Sarver, R. W., Bryant, G. L., Jr., Curry, K. A., Fairbanks, M. B., Finzel, B. C., Garlick, R. L., Heinrikson, R. L., Horton, N. C., Kelley, L.-L. C., Mildner, A. M., Moon, J. B., Mott, J. E., Mutchler, V. T., Tomich, C.-S. C., Watenpaugh, K. D., and Wiley, V. H. (1998) *Structure 6*, 923−935.
27. Ignatius, M. J., Large, T. H., Houde, M., Tawil, J. W., Barton, A., Esch, F., Carbonetto, S., and Reichardt, L. F. (1990) *J. Cell Biol. 111*, 709−720.
28. Ward, E. S., Gussow, D., Griffiths, A. D., Jones, P. T., and Winter, G. (1989) *Nature 341*, 544−546.
29. Clackson, T., Hoogenboom, H. R., Griffiths, A. D., and Winter, G. (1991) *Nature 352*, 624−628.
30. Bridges, A., Birch, A., Williams, G., Aguet, M., Schlatter, D., Huber, W., Garotta, G., and Robinson, J. A. (1995) *Mol. Immunol. 32*, 1329−1338.
31. Orlandi, R., Gussow, D. H., Jones, P. T., and Winter, G. (1989) *Proc. Natl. Acad. Sci. U.S.A. 86*, 3833−3937.
32. Kettelborough, C. A., Saldanaha, J., Ansell, K. H., and Bendig, M. M. (1995) *Eur. J. Immunol. 23*, 206−211.
33. Brooks, B. R., Bruccoleri, R. E., Olafson, B. D., States, D. J., Swaminathan, S., and Karplus, M. (1983) *J. Comput. Chem. 4*, 187−217.
34. Luque, A., Gomez, M., Puzon, W., Takada, Y., Sanchez-Madrid, F., and Cabanas, C. (1996) *J. Biol. Chem. 271*, 11067−11075.
35. Luque, A., Sanchez-Madris, F., and Cabanas, C. (1994) *FEBS Lett. 346*, 278−284.
36. Tozer, E. C., Liddington, R. C., Sutcliffe, M. J., Smeeton, A. H., and Loftus, J. C. (1996) *J. Biol. Chem. 271*, 21978−21984.
37. Tuckwell, D. S., and Humphries, M. J. (1997) *FEBS Lett. 400*, 297−303.
38. Lin, E. C. K., Ratnikov, B. I., Tsai, P. M., Gonzalez, E. R., McDonald, S., Pelletier, A. J., and Smith, J. W. (1997) *J. Biol. Chem. 272*, 14236−14243.
39. D'Souza, S. E., Haas, T. A., Piotowicz, R. S., Byers-Ward, V., McGrath, D. E., Soule, H. R., Cierniewski, C., Plow, E. F., and Smith, J. W. (1994) *Cell 79*, 659−667.
40. Dickeson, S. K., Bhattacharyya-Pakrasi, M., Mathis, N. L., Schlesinger, P. H., and Santoro, S. A. (1998) *J. Biol. Chem. 37*, 11280−11288.
41. Humphries, M. J. (1996) *Curr. Opin. Cell Biol. 8*, 632−640.
42. Landis, R. C., Bennet, R. I., and Hogg, N. (1993) *J. Cell Biol. 120*, 1519−1527.
43. Huang, C., and Springer, T. A. (1997) *Proc. Natl. Acad. Sci. U.S.A. 94*, 3162−3167.
44. Zhang, L., and Plow, E. F. (1996) *J. Biol. Chem. 271*, 29953−29957.

BI982860M